https://doi.org/10.5194/egusphere-2025-3253
Preprint. Discussion started: 15 July 2025

Characterization of a High Detection-Sensitivity Atmospheric Pressure Interface Time-of-Flight Mass Spectrometer

Fabian Schmidt-Ott[1,2], Anne Maisser[1], Alexandros Lekkas,[3] Dimitris Papanastasiou[3], George Biskos[1,4]

[1] *Climate and Atmosphere Research Centre, The Cyprus Institute, 2121 Nicosia, Cyprus*
[2] *Institute for Atmospheric and Earth System Research, University of Helsinki, 00014, Helsinki, Finland*
[3] *Fasmatech Science and Technology SA, TESPA Lefkippos, NCSR Demokritos, 15310 Athens, Greece*
[4] *Faculty of Civil Engineering and Geosciences, Delft University of Technology, 2628 CN, Delft, The Netherlands*

Correspondence to: Fabian Schmidt-Ott (f.schmidt-ott@cyi.ac.cy) or George Biskos (g.biskos@cyi.ac.cy or g.biskos@tudelft.nl)

Abstract. We have characterised a new Atmospheric-Pressure-interface Time-of-Flight Mass Spectrometer, equipped with an octapole ion trap for accumulating the sampled ions before orthogonally accelerating them into the mass analyzer. The characterisation has been carried out using ion standards produced by electrospray ionisation and mobility-selected by a differential mobility analyzer operated at atmospheric pressure. Our results show that the detection sensitivity (or limit of detection) of the mass spectrometer is in the parts per quintillion (i.e., 10^{-3} ppq; parts per quadrillion) range with temporal resolutions in the range of 1 second. When increasing the temporal resolution up to 1 minute, the detection sensitivity can be reduced to the 10 parts per sextillion (i.e., 10^{-5} ppq) range, enabling the system to measure gaseous ions of extremely low concentrations. In contrast to other mass spectrometers that employ spectra accumulation to improve the detection sensitivity for atmospheric observations, ion accumulation amplifies the signal without increasing the noise level; something that is of significant importance for probing short-lived ionic clusters during new particle formation events in the atmospheric environment, among others. We also show that the mass spectrometer has a transmission of up to 1%, and a mass resolution of 23,000 for ionic masses of ca. 600 Da., while it can offer collision-induced dissociation of the sampled ions by tuning the operating conditions of the Atmospheric-Pressure-interface stage.

1. Introduction

Time-of-Flight Mass Spectrometry (TOF-MS) has proven to be an effective method for chemical identification of species, both in field and in laboratory environments. Since its introduction in the 1940s (Stephens 1946), TOF-MS has been employed in combination with different ionization techniques and sampling interfaces, including among others Extractive Electrospray Ionization (EESI; Chen et al., 2006), Proton Transfer Reaction (PTR; Hansel et al., 1995), and Matrix-Assisted Laser Desorption/Ionization (MALDI; Karas et al., 1987), or with Atmospheric Pressure interface (APi). The latter has emerged as a specially powerful tool for measuring ionic species in gases, including the ambient air where they have proved rather valuable systems for understanding nucleation in the atmospheric environment. The APi-TOF-MS systems that have been described in the literature are manufactured by Aerodyne Research Inc. (Massachusetts, USA) and Tofwerk AG (Thun, Switzerland), having resolutions > 2000, m/z ranges up to 10.000 and transmissions that range from 0.1 to 1% depending on the mass-to-charge ratio of the sampled ions (Junninen et al., 2010; Leiminger et al., 2019).

A key challenge in using APi-TOF-MS systems in field studies of atmospheric nucleation is that their detection sensitivity (or limit of detection; LOD), which is proportional to the Signal-to-Noise Ratio (SNR), has to be high enough to detect trace concentrations of molecules that potentially nucleate to form clusters, and subsequently nanoparticles upon condensation and/or coagulation, if conditions are favourable (Kulmala et al., 2004). For instance, measuring precursor gases that play a key role in atmospheric nucleation, such as H_2SO_4, requires APi-

https://doi.org/10.5194/egusphere-2025-3253
Preprint. Discussion started: 15 July 2025

TOF-MS systems that have an LOD in the parts-per-quadrillion (ppq) range (Beck et al., 2022), whereas to be able to probe the evolution of the initial clusters they produce the required LOD has to be even below 10^2 #/cm^3 (10^{-3} ppq; Kulmala et al., 2013).

Another reason for improving the detection sensitivity of MS systems is to enable coupling with other components for elaborating the measurements, such as a Differential Mobility Analyzer (DMA; Hogan & de la Mora, 2011) that filters out a big fraction of the sampled ions based on their mobility, and/or ionisation sources that have low efficiency. For example, the ionization efficiency of $C_6H_8O_5$ by nitrate-based chemical ionization (CI) is approximately 10^{-5}% (Hyttinen et al., 2015). Combined with the inherently low concentrations of atmospheric species, requires mass spectrometers that have high detection sensitivity (i.e., low LOD) to detect them and probe their evolution in the atmospheric environment during nucleation events.

A common practice for lowering the LOD in APi-TOF-MS systems is to accumulate multiple mass spectra over extended sampling periods. In this case, the ion signal grows linearly with the number of accumulated spectra (n), while the noise increases proportionally with the square root of n. Using this approach, Kürten et al. (2011) have shown that the LOD of a CI-APi-TOF-MS, which includes a chemical ionization stage, is between 0.4 and 2.4 ppq with a T_s of 1 minute for the measurement of neutral H_2SO_4. Junninen et al. (2010) have shown that the LOD of the APi-TOF-MS system produced by Tofwerk AG is 2.4×10^{-5} ppq when the sampling time (T_s) is increased to 1 hour. Using a similar approach, Leiminger et al. (2019) reported that the LOD of the ioniAPi-TOF-MS is 2×10^{-8} ppq with the same T_s. Although such LOD values are extremely low and can thus enable detection of precursor gases in ambient air, the sampling times are too long to probe the evolution of fast-evolving species during nucleation events.

An alternative approach for lowering the LOD, or enhancing the SNR, is to physically accumulate the ions within an ion trap placed upstream of the TOF chamber, yielding a signal amplification without increasing the noise level. In fact, the SNR is linearly proportional to the accumulation time (T_a), assuming that the losses in the ion trap are negligible. This is a plausible assumption, as previous works have shown that extremely high trapping efficiencies in multipoles are possible (Pedersen et al., 2002; Xu et al., 2024). To our knowledge, the use of ion traps in APi-TOF-MS for the purpose of improving their LOD has not yet been demonstrated.

Here, we characterize a novel APi-TOF-MS, manufactured by Fasmatech, Athens, Greece, that contains an octapole ion trap, and investigate how ion accumulation within the octapole influences the detection sensitivity of the instrument. In addition, we characterize its transmission efficiency, mass resolution, and ability for controlled Collision-Induced Dissociation (CID) of species.

2. Methods

2.1 The APi-TOF-MS

The APi-TOF-MS system, the layout of which is shown in Fig. 1, has been previously described by Kaltsonoudis et al. (2023). Ions are introduced into the mass spectrometer through an capillary inlet (internal diameter of 0.5 mm) at a constant flow rate of 1.7 lpm, and guided through a series of Radio-Frequency (RF) ion guides to an orthogonal accelerator that periodically pulses them into the TOF chamber. The vacuum within the APi comprises four consecutive stages, progressively lowering the pressure by nine orders of magnitude from atmospheric levels to 10^{-6} mbar within the TOF chamber. More specifically, the APi-TOF-MS consists of an aerolens and an ion funnel, an RF octapole ion trap, an RF hexapole ion guide, a high-vacuum lens, and the TOF mass analyser.

The aerolens and ion funnel are at the first vacuum stage (1 mbar) for laminarising the under-expanded gas flow and focusing the ions through a 2-mm differential aperture, respectively, downstream the capillary inlet. Ions are confined radially by a pair of antiphase RF signals applied to the aerolens and ion funnel electrodes, with a frequency of 2.43 MHz and an amplitude of 70 V. An axial DC gradient is further applied across both elements

https://doi.org/10.5194/egusphere-2025-3253
Preprint. Discussion started: 15 July 2025

while the DC potential applied to the aperture is switched between transmission and deflection levels for gating ions further downstream (Papanastasiou et al., 2021).

Ions focused and gated through the differential aperture at the exit of the ion funnel are captured radially in an RF octapole ion guide operated at a pressure of 10^{-3} mbar, with user-defined RF frequency and amplitude $V_{RF,2}$ as specified in Table 1. This further confines and effectively guides the ion beam to the next vacuum stage of the MS. Lower RF frequencies and higher amplitudes enhance the transmission of higher m/z ions. The ion guide is segmented axially, and a weak DC gradient allows for efficient thermalization and axial transfer of the ions to downstream ion optics. The DC potential applied to the differential aperture installed at the beginning (Gate 1 Fig. 1) and the end (Gate 2) of the RF octapole, as shown in Fig. 1, can be adjusted, enabling the accumulation and subsequent release of the ion population towards the TOF mass analyser. The dual gate configuration allows both for adjusting the ion load inside the RF octapole ion guide, as well as controlling the release of ion packets towards the TOF mass analyser (cf. Fig. 1).

Ions are radially confined by an RF-only hexapole ion guide operated at 10^{-5} mbar, followed by a two-stage Einzel lens configuration coupled to a dual 2-mm slit for shaping the ion beam entering the TOF analyser. The dual Einzel lens is designed to transform the cylindrical cross-section ion beam at the exit of RF hexapole into a two-dimensional beam so that they can be accelerated by the Orthogonal Acceleration (OA) region into the TOF (Kaltsonoudis et al., 2023).

The last stage of the system is the TOF mass analyser that comprises a two-stage OA region and a two-stage reflectron operated at a flight tube energy of ~9 kV. The application of the high-voltage extraction pulses applied across the first stage of the OA is synchronized with the release of the ions from the RF octapole ion guide. To account for the mass-dependent axial spread of the ions - where heavier ions arrive into the effective region of the OA later than the lighter - multiple pulses are required to efficiently sample each ion packet having a broad m/z range of ions. This requires precise timing adjustments (i.e., the time between the release of ions from the ion trap and their subsequent orthogonal acceleration) to ensure that all m/z ions are sampled efficiently while mass discrimination effects are minimized. Ions are time-focused on a MagneTOF Electron Multiplier Detector (ETP; Sydney, Australia) operated at a gain of 1900 V. The length of the TOF chamber is ca. 2 m and the pressure is maintained at 10^{-6} mbar.

https://doi.org/10.5194/egusphere-2025-3253
Preprint. Discussion started: 15 July 2025

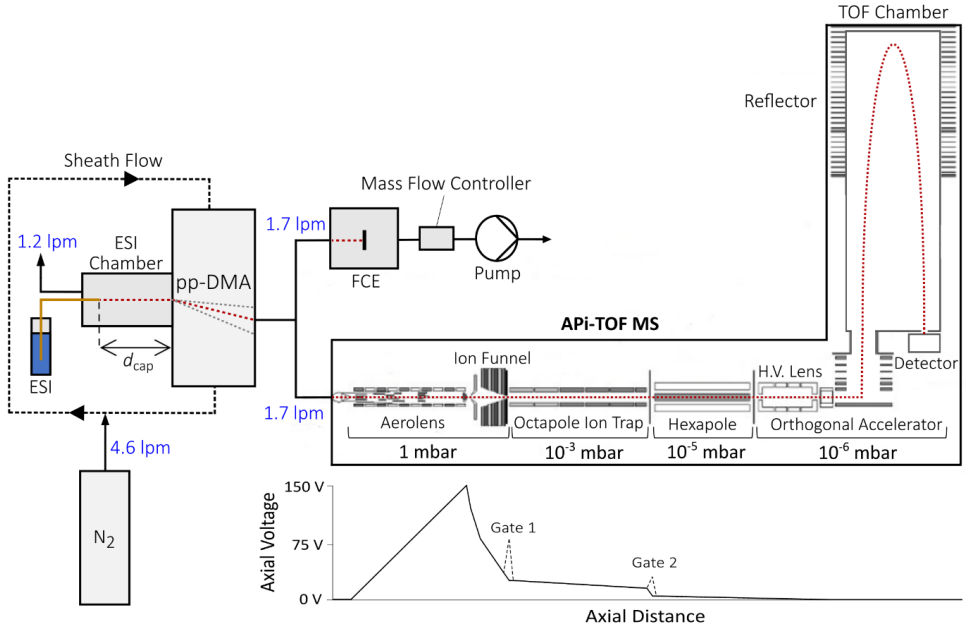

Figure 1: Schematic layout of the experimental setup and the APi-TOF-MS system. Ions were generated by ESI and mobility-selected by the pp-DMA. The resulting monodisperse ions were then directed to both a FCE and the APi-TOF-MS system. The graph shows the axial voltages applied across various stages of the APi-TOF-MS system, where gates 1 and 2 are the entrance and exit of the ion trap, respectively.

Table 1. Optimised operating configuration of the APi-TOF-MS, for high- and low-mass ranges.

Stage	Input	High-mass	Low-mass
Ion Funnel	RF	2.36 MHz	2.36 MHz
	$V_{RF,1}$	70 V	70 V
Octapole & Hexapole	RF	2.36 MHz	2.36 MHz
	$V_{RF,2}$	500 V	250 V
TOF chamber	OA timing (µs)	60, 140, 220	60, 90, 120
	MagneTOF gain	1900 V	1900 V

2.2 Measurement

Fig. 1 shows the experimental setup employed for all measurements carried out in this work. Ions having standard mobilities and masses (cf. Table 2; Ude & De La Mora, 2005) were produced using an electrospray ionization source (ESI) coupled to a parallel-plate DMA (pp-DMA; SEADM P5 DMA). The ESI was operated with a counterflow of 1.2 lpm in order to remove droplets and neutral species (Amo-González & Pérez, 2018) and was electrically floating on the pp-DMA voltage. The resolving power of the pp-DMA, determined as the full width half maximum (FWHM) divided by the peak mobility, was around 50 for the THAB monomer.

The concentration of the ions downstream the pp-DMA was measured using a Faraday Cup Electrometer (FCE; Lynx E12, SEADM), placed in parallel to the APi-TOF-MS system. The distances from the DMA and sampling flow rates of both the APi-TOF-MS system and the FCE were the same (10 cm and 1.7 lpm, respectively), ensuring

https://doi.org/10.5194/egusphere-2025-3253
Preprint. Discussion started: 15 July 2025

equal ion losses upstream the instruments. In all measurements, ion production was kept as stable as possible, with a maximum relative standard deviation of the ion concentration within 10% for different ion production rates (see Fig. S-2 in the supplement). Fragmentation within the APi-TOF-MS was minimized during measurements where it was not desired, with the fragment signal accounting for up to 3% of the signal corresponding to the original compound.

Table 2. Positively and negatively charged ions produced by ESI. Key: TPAI: tetra-methyl ammonium iodine; TPAI: tetra-propyl ammonium iodide; TBAI: tetra-butyl ammonium iodide; THAB: tetra-heptyl ammonium bromide; TDAB: tetra-decyl ammonium bromide; TDDAB: tetra-dodecyl ammonium bromide.

Species		m (Da)	Z (cm^2/Vs)
TMAI monomer	$C_4H_{12}N^+$	74.10	2.18
TMAI dimer	$(C_4H_{12}N)_2I^+$	275.10	1.48
TPAI monomer	$C_{12}H_{28}N^+$	186.22	1.62
TPAI dimer	$(C_{12}H_{28}N)_2I^+$	499.35	0.99
TBAI monomer	$C_{16}H_{36}N^+$	242.29	1.39
TBAI dimer	$(C_{16}H_{36}N)_2I^+$	611.47	0.87
THAB monomer	$C_{28}H_{60}N^+$	410.47	0.97
THAB dimer	$(C_{28}H_{60}N)_2Br^+$	899.86	0.65
TDAB monomer	$C_{40}H_{84}N^+$	578.66	0.78
TDAB dimer	$(C_{40}H_{84}N)_2Br^+$	1236.24	0.54
TDDAB monomer	$C_{48}H_{100}N^+$	690.79	0.71
Bromide ion	Br^-	78.92	N.A.
Iodide ion	I^-	126.90	N.A.
Potassium diiodide ion	I_2K^-	292.77	N.A.

The LOD of the APi-TOF-MS system is equal to the inlet concentration, at which the instrument detects a signal intensity that is equal to the signal of a single ion striking the TOF detector (S_{ion} = 60 a.u.; see Fig. S-3). The LOD can be decreased by increasing T_a inside the octapole, which effectively increases the chance that a single ion strikes the detector. In this study, T_a was varied from 0.001 to 50 s for different inlet ion concentrations ranging from 10 down to 10^{-3} ppq. Such low values were produced both by lowering the concentration of the solvent in the ESI solution down to the limit at which the ESI was still stable, and by increasing the distance between the tip of the ESI capillary and the DMA inlet (d_{cap}; see Fig. 1), effectively lowering the probability of ions passing through the DMA inlet slit through electrostatic precipitation to the frontside of the DMA inlet plate. The lowest ion concentration that could be produced by ESI was therefore limited by d_{cap} with a maximum distance of 25 mm.

To determine the mass-dependent transmission of the APi-TOF-MS, ions listed in Table 2 were generated at concentrations of approximately 0.1 ppq using a T_a in the ion trap of 0.01 s. Low ion concentrations and short accumulation times are critical for this measurement in order to minimize space-charge effects that affect transmission through the ion trap or possibly other stages within the APi-TOF-MS system. The transmission of the APi-TOF-MS is defined as the ratio between the ion count rate, expressed in ions/s, measured by the APi-TOF-MS system (I_{MS}), to that measured by the electrometer (I_{FCE}), i.e.:

$$T = \frac{I_{MS}}{I_{FCE}}, \quad (1)$$

where $I_{MS} = \frac{S}{n \cdot S_{ion} \cdot T_a}$, with S being the signal recorded by the APi-TOF-MS system and n is the number of accumulated spectra, set to 10 in all our measurements.

https://doi.org/10.5194/egusphere-2025-3253
Preprint. Discussion started: 15 July 2025

The mass-dependent resolution of the system was determined by a mass spectrum corresponding to sulphuric acid-nitrate clusters, obtained by electrospraying a methanol–ammonium sulphate solution, following the procedure described by Waller et al. (2019), as shown in Fig. S-4. The mass resolution (R) of a peak at m/z is defined as:

$$R = \frac{m/z}{FWHM}. \quad (2)$$

In a final series of measurements, we investigated the CID of THAB and TPAI dimers occurring between the ion funnel and the ion trap where the pressure is reduced from 1 to 10^{-3} mbar, which are optimal for ion fragmentation (Zapadinsky et al., 2019). We should note here that CID is used to probe the declustering strength of the sampled compounds; e.g., for assessing the compatibility of reagent ions with analyte molecules in chemical ionization (Brophy & Farmer, 2016; Lopez-Hilfiker et al., 2016). Key parameters influencing the dissociation of molecules or clusters are the type of neutral gas molecules, the kinetic energy of the ions, and the pressure within the collision cell (Sleno & Volmer, 2004). In our measurements we manipulated the ion kinetic energies to achieve a sufficient number of collisions with energies exceeding the dissociation threshold by adjusting the electric potential between those two stages (i.e., the ion funnel and the ion trap).

3. Results and Discussion

The following paragraphs provide our results and a discussion on the detection sensitivity (section 3.1), the transmission (section 3.2), and the mass resolution (section 3.3) of our APi-TOF-MS system, as well as the collision-induced dissociation (section 3.4) of clusters sampled by it.

3.1 Detection Sensitivity

Figure 2 shows the signal of the APi-TOF-MS system recorded when feeding it with different THAB monomer concentrations and accumulation times (T_a) averaged over 10 spectra. The signal increases linearly with the ion concentration up to approximately $S = 10^6$ a.u, indicating concentration-independent transmission over this certain limit for a given ionic mass. Beyond this limit, the signal plateaus for all T_a values, suggesting that space-charge effects become significant within the ion trap, leading to a maximum concentration of ions that can be accumulated (Majima et al., 2012). The space-charge limit is therefore reached either when introducing too high ion concentrations or when using an accumulation time that is too long.

The slopes of all the curves in Fig. 2 are the same, indicating that the transmission is approximately the same for all T_a values used, and suggesting that the ion trap is highly effective provided that the saturation limit is not reached. These findings are consistent with previous studies reporting that losses in multipole ion traps can be extremely low (Pedersen et al., 2002; Xu et al., 2024).

https://doi.org/10.5194/egusphere-2025-3253
Preprint. Discussion started: 15 July 2025

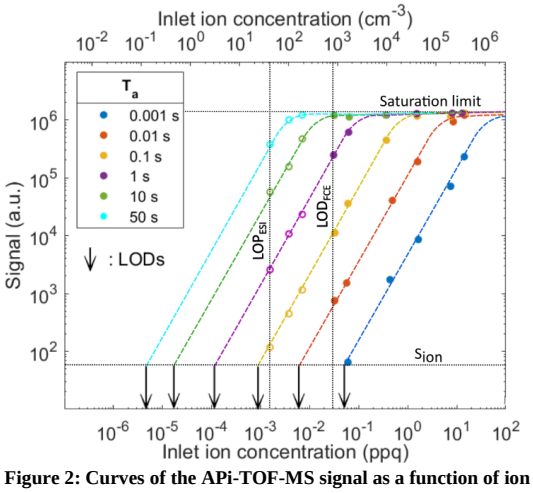

Figure 2: Curves of the APi-TOF-MS signal as a function of ion concentration at the inlet of the instrument, for different T_a within the ion trap. Solid symbols represent the measurements in which the signals from both the FCE and the APi-TOF-MS are within detection range, while the open symbols indicate measurements in which only the APi-TOF-MS is within its detection range. For the measurements reported here we used THAB monomer ions. Arrows indicate ion concentrations corresponding to the LOD for each T_a. The fitted curves for S < 10^6 are of the form $\log(S) = a \cdot log(N_{ion}) + b \cdot log(T_a) + c$, where $a = 1.56$, $b = 1.30$ and $c = 7.69$.

The limit of detection of the FCE (LOD_{FCE}) used in our setup was approximately 3×10^{-2} ppq (800 ions/cm^3). It was therefore not possible to directly investigate the LOD of the APi-TOF-MS below this concentration. However, it was possible to extrapolate inlet ion concentrations even below LOD_{FCE}, assuming that the transmission of the APi-TOF-MS is independent of concentration, and the ion concentration – signal relationship thus remains linear. The assumption that the transmission of the APi-TOF-MS remains constant even below the LOD_{FCE} is reasonable because there are no additional loss mechanisms to be expected for lower ion concentrations.

As we decreased ion concentrations even further, the limit of production of the ESI source (LOP_{ESI}) was reached at 2×10^{-3} ppq (50 ions/cm^3). Despite these extreme low concentrations, the APi-TOF-MS remained well within its detection range down to concentrations of LOP_{ESI} using an accumulation time of only 0.1 s. This demonstrates the capability to measure even lower concentrations by further increasing T_a, while maintaining temporal resolutions of a few minutes.

Figure 3 shows how the LOD of the APi-TOF-MS decreases with increasing temporal resolution (Δt), i.e., measuring time, with the lowest LOD of 3×10^{-6} ppq obtained at a temporal resolution of 500 s (8.3 minutes). This is determined as $\Delta t = n \cdot T_a$, where we accumulated a number (n) of 10 spectra to reduce uncertainties from fluctuations in ion production from the electrospray source. For atmospheric measurements in which inlet concentrations are relatively stable, Δt could practically be reduced by a factor of 10 by lowering n.

In all measurements presented here, ions of interest were selected using a pp-DMA upstream of the APi-TOF-MS. Without this filtering stage, the space-charge limit in the ion trap would be reached more quickly due to the presence of other species or the same species carrying multiple charges. This would reduce the accumulation time for the ion of interest, thereby increasing the LOD. Since this study focuses on determining the LOD of singly charged species, and given that electrospray-generated ions include multiply charged species (Gaskell, 1997), a filtering stage was necessary to ensure the selective measurement of singly charged ions. For atmospheric

https://doi.org/10.5194/egusphere-2025-3253
Preprint. Discussion started: 15 July 2025

measurements, where concentrations of different species and their ionization efficiency can vary by orders of magnitudes, it is advisable to also include such filtering system upstream of the APi-TOF-MS to prevent additional space-charge build-up within the ion trap induced by species that are not of interest.

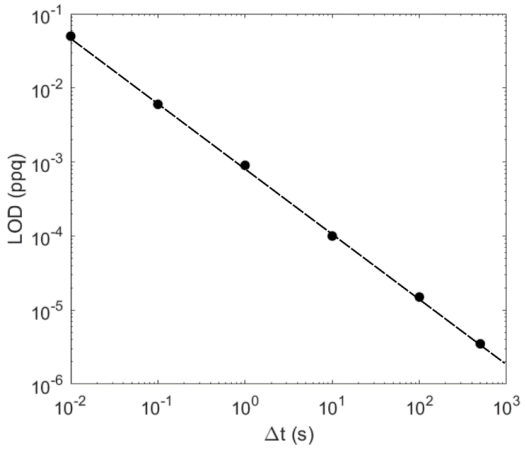

Figure 3: Minimum temporal resolutions needed for measuring ion concentrations at the lowest LOD, corresponding to the ion concentrations indicated by the arrows in Fig. 2.

3.2 Transmission

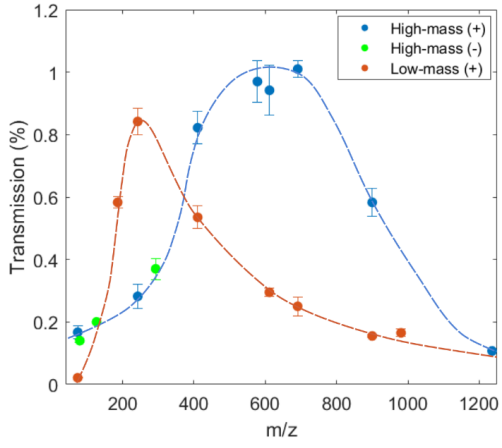

Figure 4: Mass-dependent transmission of the APi-TOF-MS system at a high-mass and a low-mass settings (see Table 1), using ion concentrations of approximately 0.1 ppq and T_a = 0.01 s.

Figure 4 shows the transmission of the APi-TOF-MS system using the high-mass and low-mass setting (cf. Table 1). For the low-mass setting, a maximum transmission of 1% was achieved at around 250 m/z for positively charged ions (see Table 2). Similar values are observed for ions of ca. 600 m/z for the high-mass setting. These results are similar to those reported for other APi-TOF-MS systems (Heinritzi et al., 2016; Junninen et al., 2010;

https://doi.org/10.5194/egusphere-2025-3253
Preprint. Discussion started: 15 July 2025

Leiminger et al., 2019). Negatively charged ions measured using the high-mass setting showed a similar trend as positively charged ions (see Fig. 4). We should note here that measurements at negative polarity were limited to only three species (Br^-, I^- and I_2K^-), because the mobility-mass calibration standards strongly fragmented at the negative ESI polarity, making them unsuitable for the study of transmission at this polarity.

The difference in the transmission distribution corresponding to the two conditions is primarily attributed to variations of $V_{RF,2}$ inside the ion trap. A higher $V_{RF,2}$ stabilizes the motion of ions with greater m/z, resulting in a transmission curve that shifts towards higher masses under the high-mass setting. The timing of the pulses in the OA was adjusted in the high-mass setting, allowing heavier ions sufficient time to reach the OA (see Fig. S-1).

3.3 Mass resolution

Figure 5 shows the resolution (R) of the APi-TOF-MS for ions produced by electrospraying a methanol–ammonium sulphate solution (see Fig. S-4). The resolution increases with mass, because heavier ions exhibit longer flight times, which enhances their separation. The lowest detectable mass was identified at 28 m/z, corresponding to C_2H_4, with a resolution of 7,000. The highest ion mass that we could produce by electrospray is at 1,244 m/z, corresponding to $(NH_3)_{35}(H_2SO_4)_{32}(H^+)_3$, with a mass resolution of 23,000. Considering that this molecule carries 3 positive charges, its molecular mass is 3,732 Da.

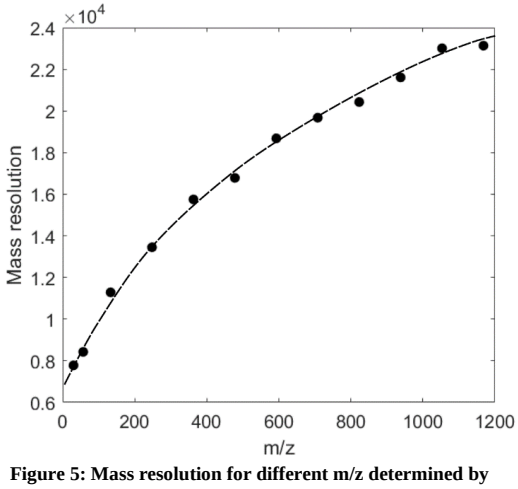

Figure 5: Mass resolution for different m/z determined by electrospraying a methanol–ammonium sulphate solution.

3.4 Collision-induced dissociation

Figure 6 shows the fraction of the signal produced by the TPAI and THAB dimers over that corresponding to the monomers and their fragments, for varying voltages applied between the ion funnel and the ion trap. The results demonstrate that CID can be controlled by tuning the voltage between those stages. Moreover, the TPAI dimer dissociates into its monomers at lower voltages than THAB, indicating that the latter is more stable with respect to CID. This is confirmed by Density Functional Theory calculations (not shown here) showing that the THAB dimer has a higher stability (1.74 eV) in comparison to the TPAI dimer (1.35 eV).

Natural bond orbital and Quantum Theory of Atoms in Molecules analysis demonstrated that the hydrogen-bromide bond within the THAB dimer is stronger than the hydrogen-iodine bond within the TPAI dimer. In these

https://doi.org/10.5194/egusphere-2025-3253
Preprint. Discussion started: 15 July 2025

calculations we assumed that the bonds connecting the monomers within the dimer involves a hydrogen atom and the respective halogen. These findings underscore that the TPAI dimer requires lower collision energies to dissociate than the THAB dimer.

Simulations by Zapadinsky et al. (2019) suggest that optimal pressures for CID in APi-TOF-MS systems lie between 10^{-2} and 1 mbar: at pressures above 1 mbar, ion-molecule collisions occur too frequently, resulting in drag forces that significantly reduce ion kinetic energy, lowering ion-molecule collision energies to values below the dissociation threshold. On the other hand, at pressures below 10^{-2} mbar the frequency of ion-molecule collisions is insufficient to obtain measurable concentrations of fragments. Thus, pressures between the ion funnel (1 mbar) and the ion trap (10^{-3} mbar) present an ideal environment for CID. By adjusting the electric potential between those two stages, it is possible to manipulate the ion kinetic energies to achieve a sufficient number of collisions with energies exceeding the dissociation threshold.

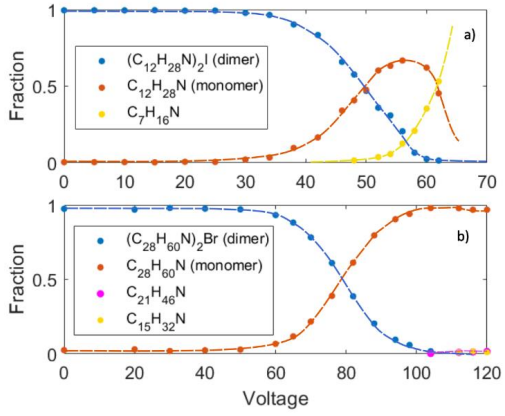

Figure 6: Fractions of the TPAI (a) and THAB (b) dimers, monomers and other fragmented species as a function of applied voltage potential between the ion funnel and the ion trap. The fraction represents the relative abundance of each species compared to the total ion population, which is proportional to their collision-induced dissociation efficiency. The dimer concentrations for both ions introduced to the APi-TOF-MS is 0.1 ppq.

4. Conclusion

We have characterized a novel APi-TOF-MS system and demonstrated its capability to measure ion concentrations down to the range of 1 part per quintillion (10^{-3} ppq, i.e., parts per quadrillion; or 25 ions/cm^3 at standard conditions), with a temporal resolution of the order of 1 second. Interestingly, the detection sensitivity can get to 1 part per sextillion (10^{-5} ppq) when the temporal resolutions is set to 1 minute, considering that the measured LOD values can be extrapolated down to that range, which is a significant improvement compared existing APi-TOF-MS systems. The high sensitivity of the system investigated here is achieved by accumulating ions within an octapole ion trap upstream the TOF chamber, resulting in amplification of the signal without an increase in noise level. This approach is advantageous compared to the conventional approaches used currently in APi-TOF-MS systems, whereby signal amplification is achieved by the accumulation of multiple mass spectra that inherently increases both signal and noise simultaneously.

https://doi.org/10.5194/egusphere-2025-3253
Preprint. Discussion started: 15 July 2025

Furthermore, we showed that the transmission of the APi-TOF-MS system is up to 1%, which is comparable to other similar mass spectrometers available on the market, and can be optimized for different masses depending on the operating conditions used. We also demonstrated that our system has a mass resolution of up to 23,000 FWHM for ionic masses of ca. 600 Da, and that the collision-induced dissociation of sampled ions can be finely controlled by adjusting the voltage potential between the funnel and ion trap within the APi.

A clear advantage of the APi-TOF-MS we investigated is its versatility, manifested by different operating settings that can be adapted to the needs. For example, when coupled with a chemical ionization source, a possible space-charge build-up from excessive concentrations of reagent ions (e.g., NO_3^-; 62 Da) inside the ion trap can be mitigated by choosing appropriate RF settings to induce a low-mass cutoff. In addition, the possibility of coupling the APi-TOF-MS system in series with a pp-DMA can allow mobility-resolved measurements of low-concentration compounds of interest while preventing space-charge build-up in the ion trap from highly concentrated species that are not relevant. Moreover, the capability for controlled collision-induced dissociation can be utilized for probing the bonding strength of those reagent ions with different types of species.

Data availability

Schmidt-Ott, F. (2025). Characterization of a High Detection-Sensitivity Atmospheric Pressure Interface Time-of-Flight Mass Spectrometer [data set]. Zenodo. 10.5281/zenodo.15854114

Author contribution

Fabian Schmidt-Ott designed and carried out the measurements and completed most of the manuscript under the guidance of Anne Maisser and George Biskos. Anne Maisser assisted in the design and measurements and provided supervisory input. Alexandros Lekkas and Dimitris Papanastasiou designed and built the APi-TOF-MS and helped to operate it for this study. George Biskos conceptualized the study, supervised the work, and provided input during the writing up of the manuscript. All authors reviewed the manuscript.

Competing Interests

The authors declare that they have no conflict of interest.

Acknowledgement

This work was supported by the NANO2LAB project that is co-funded by the European Regional Development Fund and the Republic of Cyprus through the Research Innovation Foundation (Strategic Infrastructure), as well as the ASPASIA project as part of the Research and Innovation Foundation (RIF). This work has also received funding from the from the EMME-CARE project, which is financed by the European Union's Horizon 2020 research and innovation program and the Cyprus Government.

References

Amo-González, M., & Pérez, S. (2018). Planar Differential Mobility Analyzer with a Resolving Power of 110. *Analytical Chemistry*, *90*(11), 6735–6741. https://doi.org/10.1021/acs.analchem.8b00579

Beck, L. J., Schobesberger, S., Sipilä, M., Kerminen, V.-M., & Kulmala, M. (2022). Estimation of sulfuric acid concentration using ambient ion composition and concentration data obtained with atmospheric pressure interface time-of-flight ion mass spectrometer. *Atmospheric Measurement Techniques*, *15*(6), 1957–1965. https://doi.org/10.5194/amt-15-1957-2022

Brophy, P., & Farmer, D. K. (2016). Clustering, methodology, and mechanistic insights into acetate chemical ionization using high-resolution time-of-flight mass spectrometry. *Atmospheric Measurement Techniques*, *9*(8), 3969–3986. https://doi.org/10.5194/amt-9-3969-2016

Chen, H., Venter, A., & Cooks, R. G. (2006). Extractive electrospray ionization for direct analysis of undiluted urine, milk and other complex mixtures without sample preparation. *Chemical Communications*, *19*, 2042. https://doi.org/10.1039/b602614a

https://doi.org/10.5194/egusphere-2025-3253
Preprint. Discussion started: 15 July 2025

Gaskell, S. J. (1997). Electrospray: Principles and Practice. *Journal of Mass Spectrometry*, *32*(7), 677–688. https://doi.org/10.1002/(SICI)1096-9888(199707)32:7<677::AID-JMS536>3.0.CO;2-G

Gross, J. H. (2006). *Mass spectrometry: A textbook*. Springer Science & Business Media.

Hansel, A., Jordan, A., Holzinger, R., Prazeller, P., Vogel, W., & Lindinger, W. (1995). Proton transfer reaction mass spectrometry: On-line trace gas analysis at the ppb level. *International Journal of Mass Spectrometry and Ion Processes*, *149–150*, 609–619. https://doi.org/10.1016/0168-1176(95)04294-U

Heinritzi, M., Simon, M., Steiner, G., Wagner, A. C., Kürten, A., Hansel, A., & Curtius, J. (2016). Characterization of the mass-dependent transmission efficiency of a CIMS. *Atmospheric Measurement Techniques*, *9*(4), 1449–1460. https://doi.org/10.5194/amt-9-1449-2016

Hogan, C. J. Jr., & de la Mora, J. F. (2011). Ion Mobility Measurements of Nondenatured 12–150 kDa Proteins and Protein Multimers by Tandem Differential Mobility Analysis–Mass Spectrometry (DMA-MS). *Journal of the American Society for Mass Spectrometry*, *22*(1), 158–172. https://doi.org/10.1007/s13361-010-0014-7

Hyttinen, N., Kupiainen-Määttä, O., Rissanen, M. P., Muuronen, M., Ehn, M., & Kurtén, T. (2015). Modeling the Charging of Highly Oxidized Cyclohexene Ozonolysis Products Using Nitrate-Based Chemical Ionization. *The Journal of Physical Chemistry A*, *119*(24), 6339–6345. https://doi.org/10.1021/acs.jpca.5b01818

Junninen, H., Ehn, M., Petäjä, T., Luosujärvi, L., Kotiaho, T., Kostiainen, R., Rohner, U., Gonin, M., Fuhrer, K., Kulmala, M., & Worsnop, D. R. (2010). A high-resolution mass spectrometer to measure atmospheric ion composition. *Atmospheric Measurement Techniques*, *3*(4), 1039–1053. https://doi.org/10.5194/amt-3-1039-2010

Kaltsonoudis, C., Zografou, O., Matrali, A., Panagiotopoulos, E., Lekkas, A., Kosmopoulou, M., Papanastasiou, D., Eleftheriadis, K., & Pandis, S. N. (2023). Measurement of Atmospheric Volatile and Intermediate Volatility Organic Compounds: Development of a New Time-of-Flight Mass Spectrometer. *Atmosphere*, *14*(2), 336. https://doi.org/10.3390/atmos14020336

Karas, M., Bachmann, D., Bahr, U., & Hillenkamp, F. (1987). Matrix-assisted ultraviolet laser desorption of non-volatile compounds. *International Journal of Mass Spectrometry and Ion Processes*, *78*, 53–68. https://doi.org/10.1016/0168-1176(87)87041-6

Kulmala, M., Kontkanen, J., Junninen, H., Lehtipalo, K., Manninen, H. E., Nieminen, T., Petäjä, T., Sipilä, M., Schobesberger, S., Rantala, P., Franchin, A., Jokinen, T., Järvinen, E., Äijälä, M., Kangasluoma, J., Hakala, J., Aalto, P. P., Paasonen, P., Mikkilä, J., … Worsnop, D. R. (2013). Direct Observations of Atmospheric Aerosol Nucleation. *Science*, *339*(6122), 943–946. https://doi.org/10.1126/science.1227385

Kulmala, M., Vehkamäki, H., Petäjä, T., Dal Maso, M., Lauri, A., Kerminen, V.-M., Birmili, W., & McMurry, P. H. (2004). Formation and growth rates of ultrafine atmospheric particles: A review of observations. *Journal of Aerosol Science*, *35*(2), 143–176. https://doi.org/10.1016/j.jaerosci.2003.10.003

Kürten, A., Rondo, L., Ehrhart, S., & Curtius, J. (2011). Performance of a corona ion source for measurement of sulfuric acid by chemical ionization mass spectrometry. *Atmospheric Measurement Techniques*, *4*(3), 437–443. https://doi.org/10.5194/amt-4-437-2011

Leiminger, M., Feil, S., Mutschlechner, P., Ylisirniö, A., Gunsch, D., Fischer, L., Jordan, A., Schobesberger, S., Hansel, A., & Steiner, G. (2019). Characterisation of the transfer of cluster ions through an atmospheric pressure interface time-of-flight mass spectrometer with hexapole ion guides. *Atmospheric Measurement Techniques*, *12*(10), 5231–5246. https://doi.org/10.5194/amt-12-5231-2019

Lopez-Hilfiker, F. D., Iyer, S., Mohr, C., Lee, B. H., D'Ambro, E. L., Kurtén, T., & Thornton, J. A. (2016). Constraining the sensitivity of iodide adduct chemical ionization mass spectrometry to multifunctional organic

https://doi.org/10.5194/egusphere-2025-3253
Preprint. Discussion started: 15 July 2025

molecules using the collision limit and thermodynamic stability of iodide ion adducts. *Atmospheric Measurement Techniques*, *9*(4), 1505–1512. https://doi.org/10.5194/amt-9-1505-2016

Majima, T., Santambrogio, G., Bartels, C., Terasaki, A., Kondow, T., Meinen, J., & Leisner, T. (2012). Spatial distribution of ions in a linear octopole radio-frequency ion trap in the space-charge limit. *Physical Review A*, *85*(5), 053414. https://doi.org/10.1103/PhysRevA.85.053414

Munson, M. S. B., & Field, F. H. (1966). Chemical Ionization Mass Spectrometry. I. General Introduction. *Journal of the American Chemical Society*, *88*(12), 2621–2630. https://doi.org/10.1021/ja00964a001

Papanastasiou, D., Kounadis, D., Orfanopoulos, I., Lekkas, A., Zacharos, A., Raptakis, E., Gini, M. I., Eleftheriadis, K., & Nikolos, I. N. (2021). Experimental and numerical investigations of under-expanded gas flows for optimal operation of a novel multipole differential ion mobility filter in the first vacuum-stage of a mass spectrometer. *International Journal of Mass Spectrometry*, *465*, 116605. https://doi.org/10.1016/j.ijms.2021.116605

Pedersen, H. B., Strasser, D., Heber, O., Rappaport, M. L., & Zajfman, D. (2002). Stability and loss in an ion-trap resonator. *Physical Review A*, *65*(4), 042703. https://doi.org/10.1103/PhysRevA.65.042703

Sleno, L., & Volmer, D. A. (2004). Ion activation methods for tandem mass spectrometry. *Journal of Mass Spectrometry*, *39*(10), 1091–1112. https://doi.org/10.1002/jms.703

Stephens, W. E. (1946). A pulsed mass spectrometer with time disaersion. *Phys. Rev.*, *69*, 691.

Ude, S., & De La Mora, J. F. (2005). Molecular monodisperse mobility and mass standards from electrosprays of tetra-alkyl ammonium halides. *Journal of Aerosol Science*, *36*(10), 1224–1237. https://doi.org/10.1016/j.jaerosci.2005.02.009

Waller, S. E., Yang, Y., Castracane, E., Kreinbihl, J. J., Nickson, K. A., & Johnson, C. J. (2019). Electrospray Ionization–Based Synthesis and Validation of Amine-Sulfuric Acid Clusters of Relevance to Atmospheric New Particle Formation. *Journal of the American Society for Mass Spectrometry*, *30*(11), 2267–2277. https://doi.org/10.1007/s13361-019-02322-3

Wiedensohler, A. (1988). An approximation of the bipolar charge distribution for particles in the submicron size range. *Journal of Aerosol Science*, *19*(3), 387–389. https://doi.org/10.1016/0021-8502(88)90278-9

Xu, L., Toscano, J., & Willitsch, S. (2024). Trapping and Sympathetic Cooling of Conformationally Selected Molecular Ions. *Physical Review Letters*, *132*(8), 083001. https://doi.org/10.1103/PhysRevLett.132.083001

Zapadinsky, E., Passananti, M., Myllys, N., Kurtén, T., & Vehkamäki, H. (2019). Modeling on Fragmentation of Clusters inside a Mass Spectrometer. *The Journal of Physical Chemistry A*, *123*(2), 611–624. https://doi.org/10.1021/acs.jpca.8b10744